ATLAS DETECTOR OVERVIEW AND PROGRESS

J.D.DOWELL
School of Physics and Astronomy, University of Birmingham, Birmingham B15 2TT, UK
E-mail: jdd@hep.ph.bham.ac.uk

On behalf of the ATLAS Collaboration

A brief outline is given of the physics goals and the conceptual design of the ATLAS detector at the Large Hadron Collider together with some details of the collaboration composition and project management. Each of the sub-detector systems and their performance are are then summarised and the state of progress towards final construction discussed.

1 Introduction

ATLAS is a general purpose detector for proton-proton collisions at the CERN Large Hadron Collider (LHC). The basic design parameters [1] have been chosen to allow the efficient detection and precise measurement of a variety of phenomena (Higgs Boson, Supersymmetry, Heavy Vector Bosons, Top Quark, CP violation in b-decays, Search for Compositeness) up to the maximum achievable limits. The required characteristics, determined from detailed studies of these processes and their backgrounds, are summarised in Table 1. Other talks in this conference [2] deal with the performance of ATLAS for top and electroweak physics, SUSY and Higgs searches. The aim of this paper is to outline the main features of the detector and to review the technical progress as we enter the production phase. Detailed information is available in a number of Technical Design Reports (TDRs).

In October 1998, the ATLAS Collaboration consisted of 146 institutions from 34 countries with a total of about 1800 authors (59% from CERN member states and 41% from non-member states). By the end of the year, almost all funding agencies had signed the Memorandum of Understanding, accepting responsibility for construction of various parts of the detector.

2 Experimental Environment

The LHC will have 10 times the energy (14 TeV) and 100 times the luminosity (10^{34} cm^{-2}s^{-1}) of any previous collider. With a bunch spacing of 25 ns, there will be 23 proton-proton collisions per bunch crossing at full luminosity giving 1900 charged particles in a pseudo-rapidity interval $|\eta| < 5$. The consequences for the detector design are severe. High redundancy is required for particle detection and identification, with high granularity in space and time. Even more demanding is the need for components to be radiation hard, the innermost parts having to withstand fluences of charged and neutral particles up to $\sim 10^{15}$ cm^{-2} and ionising radiation doses up to $\sim$ 30 MRad over a period of 10 years.

Table 1. Summary of Requirements

Detector Component	Required Characteristics	η coverage Measurement	Trigger
Electromagn. Calorimetry	$\sigma_E/E \approx 10\%/\sqrt{(E)} \oplus 0.7\%$ $\sigma_\theta \approx 50$ mrad$/\sqrt{(E)}$ (GeV) $\gamma - \pi^0$, γ-jet, e-jet, τ-jet separation b-tagging with electron	precision region ± 2.5 full coverage ± 3.2	± 2.5
Hadronic Calorimetry	$\sigma_E/E \approx 50\%/\sqrt{(E)} \oplus 3\%$ granularity $\Delta\eta \times \Delta\phi = 0.1 \times 0.1$ $\sigma_{E_T}/E_T < 10\%$ for $E_T > 100$ GeV granularity $\Delta\eta \times \Delta\phi = 0.2 \times 0.2$	± 3 $3 < \lvert\eta\rvert < 5$	± 3 $3 < \lvert\eta\rvert < 5$
Inner Detector	30% at $p_T = 500$ GeV 1-2% at 20 GeV efficiency > 95% for tracks with $p_T > 5$ GeV (fake < 1%) electron identification + trigger τ and b tagging secondary vertices (low L)	± 2.5	± 2.5
Muon system	10% at $p_T = 1$ TeV in stand-alone mode at high L efficiency > 95% for tracks with $p_T > 5$ GeV (fake < 1%)	± 2.7	± 2.4

3 Detector Concept

Figure 1 shows a cut-away view of the ATLAS detector [1]. Its special characteristic is the ability to make stand-alone, precision measurements of muons by using an air-cored superconducting toroidal magnet system surrounding the calorimeters, with three muon detection stations, thus providing a safeguard against possible malfunction of the inner tracker at the highest luminosity (e.g. for Higgs $\rightarrow 4\mu$).

The electromagnetic calorimeters use liquid argon as the active medium to guarantee radiation hardness, and extend to $|\eta| = 5$ to provide hermiticity for missing E_T measurements. The physics goals, however, can be met by precision measurements of leptons and jets up to $|\eta|$ around 2.5. The barrel hadronic calorimeter consists of scintillator tiles sandwiched between iron plates in an unusual configuration in which the planes of the tiles point towards the beam axis. The radiation is low enough not to cause any damage and the solution is more cost-effective than using liquid argon throughout, without loss of performance. The scintillator barrel extends over the full length of the calorimeters including the hadronic end-caps

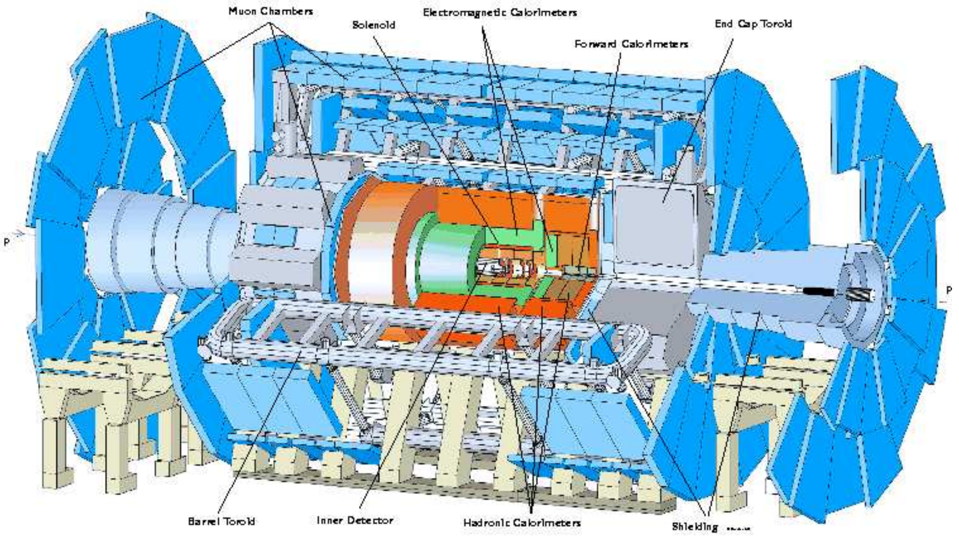

Figure 1. A cut-away view of the ATLAS detector.

which use liquid argon because of the higher radiation levels near to the beam.

The inner detector has to provide precise momentum measurements of charged particles that are contained in the calorimeters. In particular, it has to to distinguish the sign of the charge of electrons at around 500 GeV/c. A 2T superconducting solenoid magnet gives the required magnetic field. Track recognition is provided by the Transition Radiation Tracker (TRT) consisting of straw tubes which give a bubble chamber like image in the outer region of the inner detector with enhanced electron identification. These tracks are extrapolated into the inner volume where precision measurements rely on four layers of barrel silicon microstrip detectors with nine end-cap wheels on each side (SCT), and three layers of barrel Pixel detectors with 2x4 end-cap discs which also provide b-tagging.

The first level trigger makes use of energy deposits in the calorimeters and additional muon trigger chambers. It can trigger on isolated electromagnetic showers, hadronic jets, and missing E_T, and on low p_T and high p_T muons.

4 Project Approval and Management

General approval for construction, based on TDRs, has been given by the CERN Director General, advised by the LHC Experiments Committee, for the Calorimeters, Muon Spectrometer, Inner Detector, Magnets and First Level Trigger.

Within ATLAS, each detector system or sub-system is subjected to a series of System Reviews, Design Reviews, and Production Readiness Reviews (PRRs) before entering the production phase, to ensure that the detector as a whole will fit together and that viable methods have been established for each production task. Around 1000 milestones have been defined and these will constitute the main management tool for monitoring construction progress. A key milestone is the start of the detector installation in the experiment cavern at the LHC at the beginning of 2003. Work has started in 1998 on the site preparation for ATLAS at Point-1 of the accelerator ring [3], and is progressing well.

5 The Sub-detector Systems and their Status

5.1 Magnets

The ATLAS superconducting magnet system [4] consists of a central solenoid of 2T, a barrel toroid, and two end-cap toroids. Each of the toroids consists of 8 coils arranged symmetrically about the beam axis. The barrel coils will be the largest ever built, measuring 25m $\times$ 5m. There are 120 turns per coil and the operating current is 20.5 kA. The field is non-uniform with an average $\int Bdl$ of around 3 Tm. The end-cap toroids measure 9m $\times$ 5m with 116 turns per coil and 20 kA operating current producing an average $\int Bdl$ of around 6 Tm. The solenoid has a diameter of 2.5m and is 5.3m long with 1173 turns and an operating current of 7.6 kA.

The technical specifications of the toroid cold masses are complete and contracts have been placed for the conductor, coil casings and vacuum vessels. A winding machine has been installed for the barrel toroid coils. Some initial problems in producing the conductor have been overcome and there are two suppliers. A consequence, however, has been a delay of a few months in the production of the 1/3 length barrel test coil (B0). Nevertheless, the production planning still meets the installation schedule. The end-cap toroids are less critical.

Progress with the solenoid is very satisfactory. The support cylinder is complete, the conductor meets the specification and has already been used in a model coil.

The installation of a magnet test area at CERN is proceeding well.

5.2 Transition Radiation Tracker (TRT)

The inner detector [5] (radius 1.15 m) is able to make precision measurements up to $|\eta| = 2.5$ as required. The 4mm diameter straw tubes of the TRT provide up to 36 points per track, allowing excellent pattern recognition. Electron identification capability is provided by the use of Xenon gas to detect transition radiation X-rays generated in plastic foils between the tubes. This is valuable at low p_T and may be used in the Level-2 trigger. Drift time measurements give a precision of 170-200 μm per straw which allows a track to be located to 50 μm at its mid point (including systematic errors). Two discriminator thresholds are used to distinguish transition radiation hits from normal tracking hits. Pion rejection in the region of 100 (averaged over η) can be obtained for an electron efficiency of 90%.

PRRs were completed in 1998 for the barrel and end-cap mechanical aspects and full construction will start in 1999. The front-end electronics has been submitted in a radiation-hard bipolar process.

5.3 Semiconductor Central Tracker (SCT)

The SCT barrel uses four layers of silicon microstrip detectors with 80 μm pitch to provide precise coordinates in Rϕ [5]. The z-measurement is obtained using a small stereo-angle between single-sided back-to-back detectors. A barrel detector module measures approximately 12cm $\times$ 6cm and is composed of four individual wafers each with 768 strips. The resolution is 16 μm in Rϕ, 580 μm in z, and the two-track resolution is 200 μm. Similar precision is achieved in the end-caps. The total number of modules is 4088.

A crucial issue is the performance of the detectors after irradiation (total fluence 2 10^{14}cm^{-2} 1-MeV equivalent neutrons). Type inversion occurs and the detectors need a higher voltage for full depletion. p-on-n detectors have been chosen for reasons of cost, in spite of requiring a higher voltage ($\sim$300V) than n-on-n. In order to reduce the effects of radiation damage, the SCT will be operated at -7^{0}C or below. Evaporative cooling for the SCT and Pixels is under development.

Good progress has been made on prototype detector modules, hybrid readout circuits and support structures. Rad-hard optical readout, suitable also for the Pixel detectors, has been successfully tested. More critical are the front-end electronics chips. Two variants of a 128-channel, radiation hard binary readout scheme have been developed with the latest iterations submitted early in 1999. Delays in finalising the electronics mean that it is necessary to regain some months in the overall production schedule. A PRR for the modules is planned for late 1999.

5.4 Pixel Detector

The Pixel detector [5] consists of three barrels at radii of 4 cm, 11 cm, and 14 cm and four discs on each side, and uses n$^+$-on-n silicon. The innermost (removeable) pixel layer is important for b-tagging ($\epsilon_b \sim 30 - 50\%$) both for B-physics in the early running and for later Higgs and supersymmetry searches. The impact parameter resolution in Rϕ can be parametrised as $\sigma(d) = 11 + 60/\mathrm{p}_T\sqrt{(sin\theta)}$ μm.

There are approximately 1500 identical barrel modules amd 1000 identical disc modules of similar design. Each barrel module is 62.4 mm $\times$ 22.4 mm with 61440 pixel elements read out by 16 chips, each serving an array of 24 $\times$ 160 pixels. In all, there are 140M 50 μm $\times$ 300 μm detector elements, providing the fine granularity needed to cope with the high particle fluxes. The innermost layer will have to stand integrated neutron fluences of up to 3 10^{15} n cm^{-2} and up to 30 MRad.

Good progress has been made on prototype modules and supports. The charge collection is above 20,000 electrons for a minimum ionising particle, comfortably exceeding the electronics threshold of 2000 electrons, and the detectors are radiation hard to 10^{15} n cm^{-2}. Bump bonding of the detectors to the readout electronics has been mastered in several industries. The rad-hard electronics will be a critical item for 1999.

5.5 The Liquid Argon Calorimeters

The electromagnetic, end-cap hadronic and forward calorimeters [6] use liquid argon as the active medium and each has three samplings in depth. There is also a presampler for $|\eta| < 1.8$ to correct the energy measurement for showers initiated in the coil or cryostat walls. Their performance is described in [7].

The electromagnetic calorimeters ($|\eta| < 3.2$) use the accordion geometry with lead absorbers of 24-26 X_0 and copper on kapton electrodes. This technique allows the electrodes to be shaped to provide pointing towers of any desired granularity. The first 4.3 X_0 of the barrel have $\Delta\eta \times \Delta\phi = 0.003 \times 0.1$, the next 16 X_0 have 0.025×0.025 and the last sampling 0.025×0.05. The energy and angle resolutions (Table 1) are needed to achieve a mass resolution of $\sim$1% for $H \rightarrow \gamma\gamma$ and $H \rightarrow 4e$ in the mass range 90-180 GeV. The thin strips in η in the first sampling allow a π^0 rejection of > 3 at 50 GeV E_T, and provide γ direction measurements for $H \rightarrow \gamma\gamma$. Beam tests on realistic prototypes have demonstrated the required energy resolution up to 300 GeV [7].

The absorber production and stacking procedures have been successfully mastered with the required precision for both the barrel and end-cap pre-production prototypes. Problems with the industrialisation of the Cu/kapton electrodes have introduced some delay and they are now on the critical path. The barrel and end-cap cryostats have been ordered and two firms are able to produce the pin carriers for the high-voltage and signal feedthroughs. Prototypes of the presamplers have been successfully tested. Overall, the final delivery date is still on schedule.

The LAr hadronic end-caps ($1.5 < |\eta| < 3.2$) have copper absorbers perpendicular to the beam axis, the first two samplings having 25 mm thick plates and the third 50 mm, with a total absorber thickness of 12 λ. The forward calorimeter ($3.0 < |\eta| < 4.9$) is integrated into the same cryostat. The first sampling is of copper and the second and third of tungsten giving 9 λ followed by a copper plug. Because of the high particle density, the LAr gaps are very narrow (250-500 μm) to reduce the build-up of positive ions and are formed from rods parallel to the beam axis inserted into a matrix of tubes. Successful beam tests demonstrating the required performance have been carried out on pre-production versions of both the end-cap hadronic and forward calorimeters and production has been launched.

The electronics is progressing well for all the LAr calorimeters.

5.6 Scintillator Tile Hadronic Calorimeter

The range $|\eta| < 1.6$ is covered by the iron-scintillator calorimeter [8]. There is a central barrel and two extended barrel sections with partially instrumented gaps through which the services for the inner detector and LAr calorimeters pass. The tiles and iron plates are staggered in successive depth layers and the readout is by wavelength shifting optical fibres which are grouped to form approximate pointing towers. There are three depth samplings, 1.4, 4.0, and 1.8 λ thick, giving a total calorimeter thickness of 9.2 λ at $\eta = 0$. Beam tests of a combined LAr/Tile set-up have given a performance for pions up to 300 GeV/c better than required[7].

The scintillator and optics PRRs were passed in 1998 and those for the photomultipliers and electronics are due early in 1999. Mechanical construction has started with over 80% of the steel cut and delivered to the 10 production sites.

5.7 *Muon Spectrometer*

The parameters of the stand-alone muon system [9] have been optimised to detect the Standard Model and supersymmetric Higgs and new vector bosons. The momentum resolution is typically 2-3% over most of the $|\eta|$ range up to 2.7, except above 200 GeV/c where measurement and alignment errors begin to dominate, reaching 10% at $p_T = 1$ TeV. The error on a 130 GeV effective mass of 4μ is 2 GeV.

The bulk of the volume is instrumented with self-calibrated Monitored Drift Tubes (MDT) 3 cm in diameter, each having a resolution of typically 80 μm using an Ar-CH_4-N_2 mixture at 3 bar. The inner station has 2x4 layers of tubes each, and the outer two 2x3 layers to improve the accuracy and provide redundancy. Near the beam axis, $|\eta| > 2$, cathode strip chambers (CSC) are used to cope with the higher particle fluxes. They are multi-wire proportional chambers with cathode strip readout. The required resolution (60 μm) is obtained by interpolation between the 5 mm pitch strips. They are arranged in 2×4 layers per station and use an Ar-CO_2-CF_4 gas mixture. There are 370,000 MDT channels and 67,000 CSC channels. A crucial item is the optical alignment system (RASNIK) which has been demonstrated in a cosmic ray set-up and is able to correct sagitta to 6 μm (rms) even after misalignments of up to 2 mm have been introduced. The performance of the CSCs has been successfully tested at high rates using an intense ^{60}Co source together with beam particles. The MDTs are undergoing a PRR and there is some delay in constructing the pre-production chambers which it is planned to recover from the schedule. The CSCs have a PRR early in 1999.

Triggering is provided by Resistive Plate Chambers (RPC) for the barrel and Thin Gap Chambers (TGC) for the end-caps. The latter are basically MWPCs with cathode strips but having an anode pitch larger than the cathode-anode distance. Correlations between two of the three stations are used for low p_T triggers (> 6 GeV/c), while all three are used for high p_T triggers (> 20 GeV/c). The chambers also provide bunch crossing identification. There are 350,000 RPC channels and 440,000 TGC channels. Both types of chamber perform well with stable operating conditions. The TGCs are in production, having passed radiation tests. The PRR for the RPCs is in early 1999.

5.8 *Trigger and Data Acquisition*

In addition to the muon triggers from the RPCs and TGCs, the hardware based Level-1 trigger [10] uses reduced granularity data from the calorimeters and operates with a latency of 2μs, also identifying the bunch crossing that caused the trigger. It reduces the full event rate of 10^9 Hz to about 100 kHz. Regions of interest (ROI) are defined by Level-1 that contain isolated high p_T electrons or photons, jets or muons, and are used by the Level-2 trigger (latency 10 ms) to limit the amount of full granularity data it processes to reduce the trigger rate to 1 kHz. Full data are then passed to the Event Builder and further processed by a Level-3 farm, where full reconstruction is possible, to produce an output data rate of 10-100 Mbytes/s with an event rate of typically 100 Hz.

The Level-1 Calorimeter and Muon Trigger TDR was approved in September 1998 so that construction can begin. A Level-2 pilot project is scheduled for completion by the end of 1999 when the basic architecture for higher level triggers will be chosen. Final technology choices will not be made until mid-2001 when the TDR for the higher level triggers and data acquisition will be submitted.

6 Off-line Computing

The main issue is the transition from Fortran, which is heavily used for performance studies, to modern object-oriented software. This topic is covered in a separate talk[11], and has been the subject of LHCC and ATLAS internal reviews. More details can be found in the Computing Technical Proposal[12].

7 Conclusion

No major problem has been encountered in the prototyping phase of the ATLAS sub-detectors, confirming the viability of the chosen detection methods. All of the sub-detectors have already entered or are about to enter the construction phase. It should be possible to recover delays introduced by difficulties in realising some components and it is planned to complete the full detector for data taking in 2005.

Acknowledgments

I would like to thank the conference hosts for their impeccable organisation and excellent hospitality. I have benefitted from similar presentations on ATLAS by T. Akesson, A. Henriques, and P. Jenni to whom I am most grateful.

References

1. The ATLAS Technical Proposal for a General Purpose pp Experiment at the Large Hadron Collider at CERN, CERN/LHCC 94-43 (1994)
2. Top and Electroweak Physics from ATLAS, J. Parsons; SUSY from ATLAS, E. Nagy; Higgs (including SUSY Higgs) from ATLAS, T. Trefzger
3. ATLAS Technical Coordination Design Report, CERN/LHCC/99-01
4. ATLAS Magnet System Technical Design Reports, CERN/LHCC/97-18/19/20
5. ATLAS Inner Detector Technical Design Reports, CERN/LHCC/97-16/17
6. ATLAS LAr Calorimeter Technical Design Report, CERN/LHCC/96-41
7. ATLAS Cal. Performance Technical Design Report, CERN/LHCC/96-40
8. ATLAS Tile Calorimeter Technical Design Report, CERN/LHCC/97-42
9. ATLAS Muon Spectrometer Technical Design Report, CERN/LHCC/97-22
10. ATLAS First-Level Trigger Technical Design Report, CERN/LHCC/98-14
11. Software for CMS and ATLAS Experiments, S. Banerjee
12. ATLAS Computing Technical Proposal, CERN/LHCC/96-43